Published in final edited form as:
Mol Microbiol. 2015 February ; 95(4): 660–677. doi:10.1111/mmi.12893.

Enterococcus faecalis pCF10-encoded Surface Proteins PrgA, PrgB (Aggregation Substance), and PrgC Contribute to Plasmid Transfer, Biofilm Formation, and Virulence

Minny Bhatty[1], **Melissa R. Cruz**[1], **Kristi L. Frank**[2], **Jenny A. Laverde Gomez**[1], **Fernando Andrade**[1], **Danielle A. Garsin**[1], **Gary M. Dunny**[2], **Heidi B. Kaplan**[1], and **Peter J. Christie**[1,*]

[1]Department of Microbiology and Molecular Genetics, University of Texas Medical School at Houston, 6431 Fannin St, Houston, Texas 77030

[2]Department of Microbiology, University of Minnesota Medical School, 1460 Mayo Bldg., MMC196, 420 Delaware St., S.E., Minneapolis, Minnesota 55455

SUMMARY

Enterococcus faecalis pCF10 transfers at high frequencies upon pheromone induction of the *prgQ* transfer operon. This operon codes for three cell-wall-anchored proteins - PrgA, PrgB (aggregation substance), and PrgC - and a type IV secretion system through which the plasmid is delivered to recipient cells. Here, we defined the contributions of the Prg surface proteins to plasmid transfer, biofilm formation, and virulence using the *Caenorhabditis elegans* infection model. We report that a combination of PrgB and extracellular DNA (eDNA), but not PrgA or PrgC, was required for extensive cellular aggregation and pCF10 transfer at wild-type frequencies. In addition to PrgB and eDNA, production of PrgA was necessary for extensive binding of enterococci to abiotic surfaces and development of robust biofilms. However, although PrgB is a known virulence factor in mammalian infection models, we determined that PrgA and PrgC, but not PrgB, were required for efficient killing in the worm infection model. We propose that the pheromone-responsive, conjugative plasmids of *E. faecalis* have retained Prg-like surface functions over evolutionary time for attachment, colonization and robust biofilm development. In natural settings, these biofilms are polymicrobial in composition and constitute optimal environments for signal exchange, mating pair formation, and widespread lateral gene transfer.

Keywords

Gram-positive adhesins; conjugation; type IV secretion; biofilms; *Enterococcus faecalis*; virulence

INTRODUCTION

The *Enterococcus faecalis* conjugative plasmid pCF10 is rapidly and efficiently disseminated in response to donor cell perception of the peptide pheromone cCF10 (Dunny, 2013). Three genetic modules, residing on the ~26-kilobase (kb) *prgQ* operon and

*Correspondence to: Peter J. Christie Department of Microbiology and Molecular Genetics, University of Texas Medical School at Houston, Houston, TX 77005, Phone: 713-500-5440, Fax: 713-500-5499 Peter.J.Christie@uth.tmc.edu.

transcribed from the pheromone responsive-promoter P_Q, encode the factors necessary for i) processing of the 67.7-kb plasmid, ii) establishment of donor-recipient cell mating junctions, and iii) delivery of the DNA substrate to recipient cells. The processing module, at the distal end of the operon, codes for the DNA transfer and replication (Dtr) factors responsible for nicking the DNA strand (T-strand) destined for transfer within the origin-of-transfer (*oriT*) sequence (Chen *et al.*, 2007). The transfer module, located centrally in the operon, consists of about a dozen genes encoding the type IV secretion system (T4SS) through which the processed pCF10 substrate is delivered to recipient cells (Bhatty *et al.*, 2013). The proximal attachment module encodes three surface proteins, PrgA, PrgB, and PrgC, and a small, predicted cytoplasmic protein PrgU (Dunny, 2013). The attachment module, and specifically PrgB, mediates intercellular aggregation or clumping, a property long thought to be responsible for the observed extremely high frequency of pCF10 transfer (approaching one transconjugant per donor cell) in liquid cultures (Dunny *et al.*, 1978, Christie and Dunny, 1986, Olmsted *et al.*, 1991).

PrgB, also termed aggregation substance (AS), is presently the best-characterized member of a diverse group of surface adhesins that are often associated with T4SSs in Gram-positive bacteria (Dunny, 2013, Bhatty *et al.*, 2013). PrgB (1,305 residues) has a characteristic sortase-dependent cell wall anchoring motif (LPxTG) near its C terminus and two aggregation domains thought to bind a lipoteichoic acid (LTA) ligand originally termed enterococcal binding substance (Ebs) on the recipient cell surface (Waters and Dunny, 2001, Waters *et al.*, 2004, Chuang *et al.*, 2009). PrgB is distributed around the cell surface, except at the septum, in association with a fibrous mesh of unspecified composition (Olmsted *et al.*, 1993). Synthesis of PrgB is correlated with marked enhancement of virulence of pCF10-carrying *E. faecalis* cells in several experimental rabbit models (Rakita *et al.*, 1999, Schlievert *et al.*, 1998, Sussmuth *et al.*, 2000, Schlievert *et al.*, 2010). PrgB, like other members of the aggregation substance family, contains a tripeptide arg-gly-asp (RGD) motif of possible importance for binding to host integrins (Rakita *et al.*, 1999, Sussmuth *et al.*, 2000). Mutational analyses confirmed the importance of PrgB's aggregation domains to biofilm development on porcine heart valves and endocarditis infection in a rabbit model (Chuang *et al.*, 2009, Chuang-Smith *et al.*, 2010).

Despite the clear role of PrgB in attachment and aggregation, no studies have yet evaluated the contributions of PrgB or of the other two Prg factors to plasmid transfer. Similar to PrgB, PrgA (891 residues) is distributed around the cell surface in association with a fibrous mesh (Olmsted et al., 1993). Early studies also implicated a role for PrgA in surface exclusion by blocking redundant uptake of pCF10 from neighboring donor cells (Dunny *et al.*, 1985). PrgC (285 residues) has a large, central proline-rich repeat region characteristic of other adhesins displayed on the Gram-positive cell surface (Wastfelt *et al.*, 1996, Navarre and Schneewind, 1999), but its biological function(s) has not been characterized (Bhatty *et al.*, 2013). In this study, we defined the contributions of PrgA, PrgB, and PrgC to pCF10 transfer, biofilm formation, and virulence using the *Caenorhabditis elegans* infection model. Strikingly, we found that the Prg proteins are not required for high frequency transfer of pCF10 in liquid or solid-surface matings, but do contribute significantly to attachment and biofilm development on artificial surfaces. We propose that Prg-mediated robust biofilm

formation evolved as a dominant mechanism exploited by pCF10-carrying cells to optimize pheromone signal exchange, establish productive mating junctions, and disseminate genetic information in natural settings.

RESULTS

pCF10 transfers at high frequencies in the absence of PrgA, PrgB, or PrgC

The *prgA, prgB,* and *prgC* genes are located downstream of the P_Q promoter and upstream of the T4SS and Dtr processing genes in the *prgQ* operon (Fig. 1A). We first characterized the effects of precise in-frame deletions of the *prgA, prgB,* or *prgC* genes on plasmid transfer and, as expected, the Δ*prgB* mutation abolished pheromone-inducible cell aggregation (see below). Surprisingly, however, none of the individual *prg* deletion mutations diminished plasmid transfer in 2 h filter mating assays and only the Δ*prgB* mutation reduced plasmid transfer by approximately two orders of magnitude in liquid assays compared with pCF10 transfer (Fig. 1B). Each Δ*prg* mutant strain accumulated abundant levels of the other two encoded Prg surface proteins and the downstream-encoded T4SS subunits PrgJ and PcfC, indicating that the *prg* deletions did not exert polar effects (Fig. 1B). As observed previously (Hirt *et al.*, 2000), two immunoreactive PrgB species were detected in extracts of OG1RF(pCF10) cells, a predicted full-length 140-kDa species and a putative processed form of 73-kDa. In pCF10Δ*prgA* cells, however, only the 140-kDa species was detected, suggesting that PrgA contributes in some way to PrgB processing.

The Δ*prgB* mutation was complemented by expression of the entire *prgA-C* gene cluster from the native P_Q promoter carried on plasmid pINY1801 (P_Q::*prgA-C*; Table 1), as shown by accumulation of abundant levels of PrgB and restoration of plasmid transfer to wild-type (WT) levels (Fig. 1B). Expression of *prgB* only from the P_Q promoter (P_Q::*prgB*) also complemented the Δ*prgB* mutation, albeit less efficiently than with the P_Q::*prgA-C* expression construct. Expression from the constitutive P_{23} promoter yielded very low PrgB protein levels and failed to complement the Δ*prgB* defect in plasmid transfer (Fig. 1B). *cis*-expression of *prgB* with one or more of the *prg* surface genes from the same promoter thus appears to be important for optimal gene expression, or stability or proper display of the PrgB adhesin at the cell surface. These experiments were performed without shaking of the mating mixtures, and it is possible that settling of donor and recipient cells at the bottom of the culture tube stimulated mating pair formation and high-frequency transfer even in the absence of PrgB. However, in repetitions of these experiments in which the mating mixtures were vigorously shaken, Δ*prgB* donors delivered the mutant plasmid to recipients at frequencies comparable to those observed under static conditions. These findings firmly establish that, despite its significant contribution to cell-cell aggregation, PrgB confers only a modest increase in plasmid transfer frequencies.

In response to pheromone sensing, pCF10-carrying cells undergo a rapid burst in transcription from the P_Q promoter (Hirt *et al.*, 2005) and high-frequency plasmid transfer through the Prg/Pcf T4SS (Chen et al. 2007, Chen *et al.* 2008, Li *et al.*, 2012) . Although PrgA and PrgC did not contribute to efficient transfer of native pCF10, we were able to detect contributions of both surface proteins to transfer of an *oriT* mutant plasmid. In previous studies it was shown that a pCF10Δ*oriT* variant transfers at low levels (~10^{-5}

transconjugants per donor; Tc's/D) in overnight filter matings, presumably as a result of inefficient processing by the Dtr proteins at the defective *oriT* sequence (Fig. 1C) (Staddon *et al.*, 2006). We introduced the Δ*prgA* or Δ*prgC* mutations onto pCF10Δ*oriT* and, although the mutations did not further diminish transfer of the Δ*oriT* mutant plasmid, complementation with *prgA* or *prgC* expression plasmids resulted in elevated pCF10Δ*oriT* transfer frequencies. For example, a P_Q::*prgA* expression plasmid conferred slightly enhanced transfer of pCF10Δ*oriT*Δ*prgA*, whereas a P_{23}::*prgC* expression plasmid yielded aberrantly high levels of PrgC and appreciably enhanced transfer of the pCF10Δ*oriT*Δ*prgC* mutant plasmid in both filter and liquid matings (Fig. 1C). Most strikingly, however, complementation of the Δ*prg* mutations with the P_Q::*prgA-C* expression plasmid resulted in transfer of the pCF10Δ*oriT* variants at levels approaching WT pCF10 in both liquid and filter matings (Fig. 1C). Complementation of the Δ*prg* mutations with a P_Q::*prgB* expression plasmid did not enhance plasmid transfer (data not shown), establishing the importance of PrgA or PrgC synthesis for elevated transfer of the Δ*oriT* plasmids. We propose that pCF10Δ*oriT*-carrying donor cells are capable of generating only low amounts of the plasmid transfer intermediate and that in nature an equivalent situation might arise when cells are weakly pheromone-induced as a result of growth at low densities in aqueous environments. In these suboptimal settings, the cosynthesis of all three Prg surface proteins might confer a strong selective advantage for plasmid dissemination by promoting establishment or stabilization of mating pairs.

Deletion of the entire prgA-C gene cluster only modestly diminishes plasmid transfer

The lack of strong phenotypes associated with individual Δ*prg* mutations in otherwise wild-type pCF10 might due to functional redundancy among the Prg surface proteins. To examine this possibility, we deleted the entire *prgA-C* gene cluster. Interestingly, the pCF10Δ*prgA-C* mutant plasmid transferred at frequencies of only two orders of magnitude below that of pCF10 (Fig. 2A). Introduction of the P_Q::*prgA-C* expression plasmid restored transfer to levels approaching the wild-type plasmid, confirming that the encoded Prg proteins collectively exert only a modest effect on pCF10 transfer (Fig. 2A). The Δ*prgA-C* mutation places the T4SS genes immediately adjacent to the P_Q promoter (Fig. 1A), which could give rise to elevated gene expression, T4SS subunit production and machine assembly, and plasmid transfer. This was not the case, however, as shown by qRT-PCR and Western immunoblot analyses. Previous kinetic analysis monitoring *prgQ* transcript abundance following pheromone induction (Hirt et al., 2005; Chatterjee et al. 2013) showed a rapid rise in levels of mRNA spanning the entire operon within the first 15-30 min., followed by a decrease. Figure 2B shows a representative experiment comparing kinetics of mRNA accumulation of the Q_L region located upstream of the *prgA-C* gene cluster versus downstream protein coding genes including *prgD, prgJ, pcfC*, and *pcfG* for strains carrying pCF10 or the Δ*prgA-C* mutant plasmid. As expected, transcription of all genes tested increased to a maximum within 30 min. and leveled off or decreased within 60 min. This general pattern was seen in biological replicates from both strains, although the Δ*prgA-C* mutation reproducibly conferred diminished transcript levels for genes distal in the operon, e.g., the *pcfG* relaxase gene, compared with the corresponding regions from the WT pCF10 plasmid (Fig. 2C). Nevertheless, strains carrying pCF10 or the Δ*prgA-C* mutant plasmid accumulated the downstream-encoded Prg/Pcf proteins at comparable levels as shown by

Western immunoblotting, suggestive of prolonged stabilities of the T4SS and Dtr proteins relative to transcripts, which is consistent with previous findings (Fig. 2C; Hirt et al., 2005). In view of these findings, we conclude that the observed high frequency transfer of pCF10**Δ***prgA-C* cannot be attributed to enhanced transcription through the *prgQ* operon and elevated T4SS machine production.

Introduction of the P_Q::*prgA-C* expression plasmid into the Δ*prgA-C* mutant strain did not alter levels of PrgJ, PcfC, or PcfG, indicating that the 5' region of the *prgQ* operon encoding the *prgA*, *prgB*, and *prgC* genes also does not encode *trans*-acting regulatory factors, e.g., small regulatory proteins or RNAs, involved in modulation of downstream gene expression (Fig. 2B). However, as mentioned above, the *prgA-C* cluster codes for a small, predicted cytoplasmic protein PrgU (Fig. 1A). We have identified a number of interesting *prgU* mutant phenotypes suggestive of a role in *prgQ* regulation, but relevant to this study, we have confirmed that the Δ*prgA*, Δ*prgB*, and Δ*prgC* mutations do not affect PrgU synthesis. Introduction of a *prgU* expression plasmid into the Δ*prgA-C* mutant also does not alter phenotypes reported here for this strain (Bhatty *et al.*, manuscript in preparation).

The PrgA, PrgB, and PrgC surface proteins are therefore required for robust transfer of pCF10 at frequencies approaching 1 Tc/D, but an alternative surface adhesin(s) appears to be contribute to high-frequency transfer (10^{-2} - 10^{-3} Tc's/D) of the pCF10Δ*prgA-C* mutant plasmid. We sought to identify such an alternative adhesin(s), and to this end we quantitated pCF10Δ*prgA-C* transfer efficiencies by donor strains bearing mutations in chromosomal genes encoding various surface functions, including SrtA (housekeeping sortase), StrC (also termed Bps, biofilm and pilus-associated sortase), EbpABC (pilus proteins), quorum-activated FsrB, or FsrB-regulated surface protein Ace and proteases GelE and SprE (Fig. S1). Whereas the Δ*srtA*, Δ*srtC*, Δ*srtA*/Δ*srtC*, and Δ*fsrB* mutant strains exhibited slight reductions in pCF10Δ*prgA-C* transfer of about one log in liquid matings, the Δ*ebpABC*, Δ*ace*, Δ*gelE*, Δ*sprE*, and Δ*sprE*Δ*gelE* mutants transferred the plasmid at levels observed with the parental donor OG1RF. These chromosomally-encoded surface factors might function additively to promote transfer of pCF10Δ*prgA-C*, although further screening might identify a critical surface protein or nonprotein adhesin.

PrgB-mediated aggregation and plasmid transfer is significantly enhanced by eDNA

Because extracellular DNA (eDNA) is a well-established contributor of cellular aggregation (Liu *et al.*, 2008, Das*et al.*, 2014) and biofilm development (Flemming and Wingender, 2010, Dunny *et al.*, 2014), we sought to determine if eDNA might be important for PrgB-mediated aggregation or pCF10 transfer. As shown previously (Dunny *et al.*, 1978), OG1RF(pCF10) forms visible clumps (Fig. 3B) that result in a pronounced decline in culture optical density within 2- to 3-h after exposure to pheromone (Fig. 3A). Strikingly, the addition of DNase at the onset of the pheromone-induction period completely abolished pCF10-mediated aggregation without affecting cell viability (Figs. 3A, B). Pheromone-induced OG1RF does not aggregate (Dunny *et al.*, 1978), and the plasmid-free strain also exhibited no differences in growth or cell viability in the absence or presence of DNase. The Δ*prgB* mutant strain carrying the P_Q::*prgB* expression plasmid aggregated extensively and DNase treatment abolished aggregation without affecting cell viability, whereas the

uncomplemented Δ*prgB* strain neither clumped nor exhibited a discernible change in growth in the presence of DNase (Figs. 3A, B).

Addition of DNase to a mating mixture composed of OG1RF(pCF10) donor cells reduced plasmid transfer by approximately two orders of magnitude, which was comparable to the decrease in transfer associated with the Δ*prgB* mutation (Fig. 3C). By contrast, DNase treatments of mating mixtures composed of donors carrying the pCF10Δ*prgB* or pCF10Δ*prgA-C* mutant plasmids did not reduce the level of plasmid transfer (Fig. 3C). Treatments of mating mixtures with heat-inactivated DNase or RNase also did not disrupt pheromone-induced clumping or plasmid transfer (data not shown). PrgB thus promotes aggregation and confers a ~2-log increase in plasmid transfer by a mechanism(s) that is strongly dependent on the presence of eDNA. In a Δ*prgB* mutant, however, other surface adhesins appear to stimulate high-frequency plasmid transfer independently of eDNA.

PrgA and PrgB contribute substantially to the formation of mature biofilms

PrgB contributes to biofilm formation, as shown using an *ex vivo* model of cardiac valve colonization (Chuang-Smith et al., 2010). We extended these earlier findings by analyzing contributions of the Prg proteins and eDNA to biofilm formation on abiotic surfaces (Fig. 4). Strikingly, pheromone-induced OG1RF(pCF10) cells accumulated over an order of magnitude more biofilm biomass than plasmid-free OG1RF cells, as determined with a crystal violet (CV)-adherence assay. OG1RF cells carrying the pCF10Δ*prgA-C* mutant plasmid formed biofilms with biomasses comparable to those of plasmid-free OG1RF, whereas the Δ*prgA-C* mutant strain carrying the P_Q::*prgA-C* expression plasmid exhibited robust biofilm development (Fig. 4). OG1RF cells carrying the P_Q::*prgA-C* expression plasmid also exhibited robust biofilm development, as evidenced by pronounced CV-staining at levels even exceeding staining of the OG1RF(pCF10) biofilms (Fig. 4). Synthesis of the Prg surface proteins therefore suffices among the pCF10-encoded proteins for extensive attachment to polystyrene surfaces and robust biofilm development.

We treated cells with DNase (2U μl^{-1} final concentration) at the onset of or at 21 h following cCF10 induction and deposition of cells on polystyrene, and then we quantitated biofilm biomasses at 24 h. Addition of DNase concomitantly with pheromone strongly abrogated biofilm development over the next 24 h by strains producing the Prg proteins (Fig. 4). In contrast, DNase treatment of pCF10-carrying cells at 21 h did not disrupt established biofilms when examined at 24 h (Fig. S2). These findings suggest that eDNA contributes significantly to the initial Prg-mediated attachment phase of biofilm development, whereas its removal from established biofilms does not result in cellular detachment and dispersion.

Next, we examined the contributions of individual *prg* genes to polystyrene adherence (Figs. 4 & S2). Interestingly, deletion of Δ*prgA* or Δ*prgB* significantly attenuated biofilm development to levels comparable to that observed with plasmid-free OG1RF. DNase treatments of OG1RF or the Δ*prgA* or Δ*prgB* mutant strains resulted in slight, further reductions in biofilm biomass. Complementation of the Δ*prgA* or Δ*prgB* mutations with P_Q-expressed *prgA* or *prgB* partially restored biofilm development, and DNase treatments strongly inhibited biofilm development of the complemented strains. The Δ*prgC* mutation did not disrupt biofilm development, although interestingly the complemented strain

produced biofilms with biomasses substantially greater than those of pCF10-carrying cells. As observed with pCF10-carrying cells, DNase treatments of the Δ*prgC* mutant and complemented strain strongly disrupted biofilm development when added at the onset of cCF10 induction and cell deposition (Fig. 4), but had little effect when added at 21 h postinduction (Fig. S2). We conclude that PrgA and PrgB, but not PrgC, contribute significantly to polystyrene adherence by a mechanism that is strongly dependent on eDNA.

We also tested whether the pCF10-encoded T4SS contributes to biofilm development, for example, through release of eDNA. We first observed that T4SS mutants deficient for production of the PrgK cell wall hydrolase or VirB4-like PrgJ ATPase displayed 20 - 30 % reductions in biofilm biomasses, whereas a mutant lacking the PcfC substrate receptor exhibited only a slight reduction in biofilm biomass compared with the parental strain OG1RF(pCF10) (Fig. S2). Second, DNase treatments abolished biofilm development by all three mutant strains (Fig. S2). While the latter finding argues against the T4SS as a dominant mechanism for eDNA release, the former points to a contribution by specific T4SS components to establishment of biofilms on polystyrene surfaces.

For a more complete analysis of biofilm formation, OG1RF with the pCF10 variants were allowed to develop for 48 h on the surface of polymethylmethacrylate (PMMA) discs placed in the bottom of 24 well plates. After completion of biofilm growth, the coupons were rinsed and incubated in a mixture of hexidium iodide (HI) to stain cells and eDNA, and calcofluor white to stain extracellular polysaccharide (EPS). Fig. 5 shows merged and separated fluorescence images of biofilms stained with HI (red) and calcofluor white (green) along with quantitation of biomass thicknesses; total fluorescence intensities are presented in Table S1. Microscopic observation of the mature biofilms confirmed that OG1RF(pCF10) cells developed appreciably thicker biofilms than the plasmid-free strain. pCF10-carrying cells formed biofilms with an abundant extracellular matrix that included EPS and eDNA. The light orange color of the biofilm image in Fig. 5 reflects the relatively uniform nature of this biofilm, as the EPS and eDNA largely overlap. OG1RF(pINY1801) expressing P_Q::*prgA-C* also formed thick biofilms, although these possessed large HI- and calcofluor-staining aggregates that were not characteristically seen with the uniform OG1RF(pCF10) biofilms (Fig. 5; also see below). In contrast, plasmid-free OG1RF biofilms were considerably thinner and the matrix was composed of a relatively larger contribution of HI-staining eDNA than calcofluor-staining EPS (Fig. 5; Table S1).

The Δ*prgA*, Δ*prgB*, and Δ*prgA-C* mutant strains formed biofilms of a similar thickness to OG1RF (Fig. 5). The Δ*prgB* and Δ*prgA-C* mutants, and to a lesser extent the Δ*prgA* mutant, formed biofilms with small and evenly distributed aggregates that stained well with HI, indicative of the presence of individual cells or microcolonies and eDNA. In striking contrast, the Δ*prgC* mutant formed thick biofilms resembling those formed by OG1RF(pCF10) cells (Fig. 5; Table S1). These findings, which are consistent with results of the CV-adherence assays (Fig. 4), suggest that production of PrgA and PrgB is necessary and sufficient among the pCF10-encoded proteins for establishment of robust, mature biofilms.

The Prg proteins and eDNA contribute to early biofilm development

We next examined the contributions of the surface factors and eDNA to early biofilm development by microscopy. We detected enhanced deposition and biofilm development by pCF10-carrying cells compared with the plasmid-free strain as early as 2 - 3 h following pheromone induction, but these differences were best illustrated at 8 and 24 h post-induction (Fig. 6; Table S1). To distinguish matrix components and permeable cells from intact cells, the biofilms were first treated with GelGreen to detect the eDNA and permeable (lysed) cells (green color), and then with calcofluor white to detect EPS (blue color) and HI to detect intact cells (red color) (Tribble et al., 2012). At 8 h, OG1RF cells formed only small sporadic aggregates with an occasional larger aggregate on the substrate surface. The aggregates were composed of comparable amounts of eDNA/lysed cells, EPS, and intact cells. In contrast, even at this early time point, OG1RF(pCF10) cells attached to the entire surface and formed thick and uniform biofilms with a matrix abundant in HI-staining intact cells, GelGreen-staining eDNA and lysed cells, and calcofluor-staining EPS. These biofilms possessed considerably more GelGreen-stained foci than OG1RF biofilms, suggestive of an accumulation of lysed cells (Fig. 6, compare B panels). OG1RF(pINY1801) expressing P_Q::*prgA-C* also formed thick biofilms, although with considerably more discrete HI-staining cell aggregates than observed with the OG1RF or OG1RF(pCF10) biofilms. Another notable difference was that the OG1RF(pCF10) biofilms possessed considerably more calcofluor-staining EPS than the OG1RF and OG1RF(pINY1801) (Fig. 6, C panels; Table S1). Finally, addition of DNase at the onset of pheromone induction and cell deposition disrupted biofilm development by all three strains but most appreciably by OG1RF(pCF10).

At 24 h postinduction, all three strains developed thicker biofilms with increased amounts of cells and eDNA compared with the 8 h biofilms (Fig. 6). However, the increase in biomass was most significant for OG1RF(pCF10) biofilms and these contained considerable more eDNA/lysed cells and EPS than those of plasmid-free OG1RF (Fig. 6, compare panels B-D; Table S1). OG1RF(pINY1801) biofilms also were much thicker than those of parental OG1RF cells, although the matrix contained less EPS compared with OG1RF(pCF10) biofilms. As observed at 8-h, DNase treatment strongly disrupted biofilm development of all three strains, but was most pronounced for OG1RF(pCF10) (Fig. 6, panels E). Consistent with data presented in Figs. 4 and 5, few individual cells or aggregates were detected on the DNase-treated substrates, strongly indicating that eDNA is involved in the early attachment phase of biofilm development.

Quantitative analysis of isolated eDNA showed that OG1RF(pCF10) biofilms possessed nearly 2 and 5 times the amount of eDNA per CFU at the 8 and 24 h postinduction periods than OG1RF biofilms (Fig. S3). The progressive accumulation of eDNA and EPS by pCF10-carrying cells during the postinduction period, possibly as a result of cell lysis, thus correlates with development of robust biofilms with considerably more biomass than those of the plasmid-free strain.

PrgA and PrgC are important virulence factors in the C. elegans *infection model*

Finally, we assessed the contributions of the Prg proteins to virulence using the *C. elegans* infection model. Strain OG1RF kills adult worms within 5-10 days of exposure, and several of the chromosomally-encoded virulence factors involved in worm killing are also relevant to mammalian pathogenesis (Garsin et al., 2001). In agreement with earlier findings for PrgB-like Asa1 from plasmid pAD1 (Garsin *et al.*, 2001), cells carrying pCF10 or pCF10Δ*prgB* displayed similar levels of virulence as plasmid-free OG1RF, as evidenced by comparable LT_{50}'s (time for half of the worms to die) when worms were fed with each strain (Fig. 7A). The Δ*prgB* mutant in fact exhibited a slight, but statistically significant ($P < 0.01$) enhancement in killing compared with OG1RF or OG1RF(pCF10). By contrast, the Δ*prgA* and Δ*prgC* mutant strains exhibited strikingly reduced rates of killing throughout the infection period, as evidenced by LT_{50}'s of ˜8 days compared with 6 days for OG1RF(pCF10) ($P < 0.001$) and by survival of ~40 % of the infected worms throughout the 11-day infection period. The Δ*prgA-C* mutant was similarly attenuated in *C. elegans* killing. Complementation of the Δ*prgA*, Δ*prgC*, and Δ*prgA-C* mutations with the corresponding gene(s) expressed from the P_Q promoter restored virulence to levels observed with OG1RF(pCF10) (Fig. 7B). In this killing assay, therefore, the presence of pCF10 did not correlate with an increase in virulence of OG1RF cells, yet selective removal of PrgA or PrgC, or of dall the Prg surface proteins, resulted in attenuated virulence. Overall, these findings are reminiscent of a previous study showing that production of mutant forms of PrgB reduced colonization of heart valves below that of the Δ*prgB* mutant or even plasmid-free OG1RF cells (Chuang *et al.* 2009, Chuang-Smith *et al.*, 2010). Below, we discuss possible mechanisms by which synthesis of a subset of the Prg proteins or of mutant Prg proteins might attenuate virulence in the *C. elegans* infection model (see Discussion).

E. faecalis proliferates and causes gross distension of the worm gut within 3 days of infection, whereas nonpathogens such as *Enterococcus faecium* proliferate but do not kill the worm or *Bacillus subtilis* fail to colonize and are cleared from the gut (Garsin *et al.*, 2001, Sifri *et al.*, 2002). We tested whether the Δ*prgA*, Δ*prgC*, and Δ*prgA-C* mutant strains proliferate or are cleared from the gut by quantitating the bacterial loads in worms at 1, 3, and 5 days following infection. Interestingly, we detected no appreciable differences in CFU's between OG1RF lacking or carrying wild-type pCF10 or mutant plasmids (Fig. S4). Thus, similar to *E. faecium*, these *prg* mutant strains retain the capacity to proliferate without killing the worm.

DISCUSSION

In early studies of the *E. faecalis* pCF10 system, some Tn917 mutations in the *prgQ* regulatory region were shown to confer correlative increases in synthesis of a ˜137-kDa protein (now termed PrgB or aggregation substance), cell-cell aggregation, and pCF10 transfer (Christie and Dunny, 1986, Christie *et al.*, 1988). PrgB-mediated aggregation was thus postulated to contribute to establishment of conjugative junctions, and the general concept emerged that surface adhesins encoded by Gram-positive mobile genetic elements (MGEs) comprise the functional counterpart of conjugative pili elaborated by Gram-negative systems in mediating the initial attachment phase of mating pair formation

(Alvarez-Martinez and Christie, 2009, Bhatty *et al.*, 2013). Here, however, we discovered that neither PrgB nor the two other pCF10-encoded adhesins PrgA or PrgC are required for efficient plasmid transfer in laboratory matings. Given that many Gram-positive MGEs encode Prg-like proteins or other adhesins, we sought to identify other biological functions responsible for retention of the pCF10-encoded *prg* genes during evolution. The data support a new model in which the Prg factors function as nonspecific adhesins that coat the enterococcal cell surface and, through a complex network of interactions with matrix components, mediate formation of robust biofilm communities. Pheromone sensing and P_Q promoter induction are rapid events (Chatterjee *et al.*, 2013) that appear to provide a selective advantage for plasmid-carrying donor cells in colonization, biofilm development, and gene transfer.

One of our most striking findings was that PrgB is dependent on eDNA to promote extensive cell-cell aggregation. The biological relevance of this activity is underscored by the findings that, in addition to inhibiting cell aggregation (Fig. 3), DNase treatment blocked pCF10-mediated attachment to abiotic surfaces and biofilm development (Figs. 4, 6). DNase did not disperse previously-aggregated or -attached cells (Fig. S2), indicating that PrgB and eDNA function primarily in initial attachment reactions. Other studies have demonstrated the importance of eDNA for development of biofilms by plasmid-free enterococci (Thomas *et al.*, 2008, Barnes *et al.*, 2012, Dunny et al., 2014) and other species including *Pseudomonas aeruginosa* (Whitchurch *et al.*, 2002) and *Staphylococcus aureus* (Rice *et al.*, 2007). To our knowledge, however, this is the first identification of a protein adhesin acting in conjunction with eDNA to promote extensive aggregation and biofilm development.

In early studies, PrgB was proposed to promote aggregation through specific binding of LTA receptors on the recipient cell surface (Olmsted *et al.*, 1991, Waters *et al.*, 2004). Our present findings suggest a more complex picture whereby PrgB mediates nonspecific aggregation by establishing a network of interactions with eDNA and other matrix components. PrgB promotes formation of visible aggregates within 2-3 h of cCF10 induction, and therefore such matrix components must exist or be produced and surface-displayed within this time frame. Indeed, a recent scanning electron microscopy (SEM) study identified long strands of fibrous material termed yarn structures on the surfaces of OG1RF cells recovered from early (4 h) biofilms (Barnes *et al.*, 2012). Labeling studies confirmed these structures were composed of eDNA encased within another extracellular matrix (ECM) component, possibly LTA or EPS. There is also evidence for a contribution of divalent cations to establishment or stabilization of biofilms by both Gram-positive and -negative species (Banin et al., 2006, Cavaliere et al., 2014, Das *et al.*, 2014). In *P. aeruginosa*, for example, it was recently postulated that a combination of eDNA, divalent cations, and other charged matrix components form a network of cationic bridges and acid-base contacts that results in intercellular aggregation and biofilm development (Das *et al.*, 2014). We have not yet evaluated the role of divalent cations to PrgB-mediated aggregation, but charge-based interactions are likely important given that EDTA treatment rapidly disperses pheromone-induced cell aggregates (Dunny *et al.*, 1978). Thus, a reasonable working model is that upon pheromone induction the surface display of PrgB and associated matrix components alters surface charge, hydrophobicity and other physico-chemical

properties of pCF10-carrying enterococcal cells, resulting in rapid and extensive aggregation.

We gained several lines of evidence that PrgB physically and functionally interacts with PrgA. First, it is noteworthy that the start-site for *prgB* overlaps with the 3' end of *prgA* (Hirt *et al.*, 2005); this genetic linkage is conserved for *prgA*- and *prgB*-like gene pairs on many different *E. faecalis* pheromone-dependent plasmids or chromosomal MGE's or pathogenicity islands (Christie, P.J., unpublished observations). Such a linkage is highly suggestive of translational coupling, which can serve to ensure the coordinated synthesis of interacting protein partners (Lovdok *et al.*, 2009). Correspondingly, we determined that coexpression of *prgA* and *prgB* from the same promoter was necessary for accumulation of PrgA and PrgB at abundant levels and for complementation of the Δ*prgA* and Δ*prgB* mutations (Fig. 1). Second, we observed that PrgA synthesis was correlated with the accumulation of a ~73-kDa PrgB species, presumptively arising from proteolytic degradation of the full-length, ~140-kDa form. We do not yet know the function of the ~73-kDa species, but recently determined that it accumulates almost exclusively in the extracellular milieu, suggestive of active proteolytic release from the cell surface (Fig. 1 & data not shown). Third, we showed that while synthesis of PrgB alone promotes cell-cell aggregation, cosynthesis of both PrgA and PrgB is required for efficient attachment of enterococcal cells to artificial surfaces and for robust biofilm development (Figs. 4-6). In light of these findings, it is noteworthy that PrgA also was reported to function as a surface exclusion factor (Dunny *et al.*, 1985). PrgA thus appears to function dually, on the one hand by antagonizing PrgB-mediated aggregation and plasmid transfer when the two proteins are produced on separate donor cells, and on the other by coordinating with PrgB to promote attachment to surfaces and development of robust biofilms when the two proteins are cosynthesized on the same donor cell. The mechanism by which PrgA modulates PrgB's adhesin functions remains an intriguing question for further study.

Finally, the early microscopy studies showing colocalization of PrgA and PrgB on hair-like projections surrounding the cell surface are consistent with the notion that PrgA and PrgB form a functional adhesin complex (Olmsted *et al.*, 1993). Our *in silico* structural analyses of PrgA and PrgB provided further support for this proposal, wherein PrgA (891 residues) adopts a predicted extended α-helical secondary structure along its entire length and has several predicted coiled-coil motifs; these structural features might contribute to fiber formation and multimerization. More intriguingly, we determined by Phyre 2.0 modeling (Kelley and Sternberg, 2009) that PrgB (1,305 residues) is a structural homolog along its entire length with *Streptococcus mutans* antigen I/II (PrgB residues 191-626: 22% identity, 100 % confidence, fold library ID c3ipkA; residues 749-1225: 28% identity, 100 % confidence, fold library ID c3qe5A). This finding is of considerable interest because *S. mutans* I/II antigen, also termed adhesin P1, recently was shown to be an amyloid-forming protein that contributes to biofilm formation (Oli *et al.*, 2012).

Our finding that pCF10-carrying cells rapidly accumulate abundant amounts of eDNA and EPS during biofilm development suggested the possibility of a dedicated, plasmid-encoded release or secretion mechanism(s). We gained some evidence that the T4SS contributes to biofilm formation (Fig. S2), which warrants further investigation, but our studies with strain

OG1RF(pINY1801) (Figs 4-6, Table S1) strongly suggested that the *prgA* and *prgB* gene products are predominantly responsible among the pCF10-encoded proteins for rapid and robust biofilm development. The *prgA-C* gene cluster might function as a delivery system for matrix components, but it seems more likely that the Prg factors form a fibrous mesh that simply provides a stratum for binding and accumulation of matrix components released by another chromosomally-encoded pathway(s). Another interesting possibility, in line with earlier studies establishing the importance of autolysis as a source of matrix components during early biofilm development (Thomas *et al.*, 2008), is that *prgA-C* expression contributes to release of matrix components by promoting lysis of a subpopulation of donor cells. In support of this model, previously it was shown that a subpopulation of pCF10-carrying cells grown in biofilms exhibited both an increase in plasmid copy number and aberrantly high expression from the P_Q promoter (Cook *et al.*, 2011, Cook and Dunny, 2013). Here, we further observed that pCF10-carrying cells form early biofilms with appreciably greater numbers of lysed cells than biofilms composed of plasmid-free cells. In response to pheromone sensing and early during biofilm development, therefore, a subpopulation of pCF10-carrying cells would experience enhanced plasmid copy number and expression of the *prgQ* operon at aberrantly high levels, the latter either as a result of stochastic transitions in the regulatory circuitry or sensing of localized, high concentrations of inducing pheromone in microcolonies. These cells would overproduce the Prg adhesins and, possibly, the T4SS machinery, which in turn leads to a disruption of cell envelope integrity and, ultimately, cell lysis. Pheromone-induced dysregulation of Prg protein synthesis and autolysis by a subpopulation of donor cells would thus provide the source of abundant matrix components utilized by remaining viable cells for robust biofilm development.

In the *C. elegans* infection model, pathogenic organisms such as *E. faecalis* infect and proliferate in the lumen of the worm's intestine inciting death within 5-6 days (Garsin *et al.*, 2001). Several *E. faecalis* virulence factors, such as cytolysin and Fsr quorum-regulated gelatinase and serine protease, have been shown to contribute both to *C. elegans* killing as well as vertebrate infection (Garsin *et al.*, 2001, Sifri *et al.*, 2002). However, other chromosomally-encoded surface adhesins shown to contribute to virulence in the mammalian systems, such as Esp, Ace, and EbpA, do not promote *C. elegans* killing, possibly because of functional redundancy or differences in host factors (Qin *et al.*, 2001, Singh *et al.*, 2010, Garsin *et al.*, 2014). Here, we found that OG1RF strains lacking and carrying pCF10 incited similar rates of worm killing (LT_{50}'s of ~6 days), but the Δ*prgA-C*, Δ*prgA* or Δ*prgC* mutations conferred significantly attenuated virulence in this model. The PrgA and PrgC proteins might mediate interactions with specific factors within the worm host that are important for attachment, colonization and/or proliferation, or they could contribute to evasion of the innate immune response. Indeed, an effect of the Δ*prgA* mutation on attachment and colonization seems highly likely in view of our finding that the Δ*prgA* mutant strain readily forms multicellular aggregates but does not attach efficiently to surfaces or form robust biofilms (Figs. 4-6).

Alternatively, the attenuated virulence phenotypes of the Δ*prgA* and Δ*prgC* mutations might be attributable not to the absence of the corresponding Prg factors *per se*, but to the resulting

assembly of a dysfunctional surface complex composed of the remaining Prg proteins. This proposal derives from earlier work using heart valve colonization models in which it was shown that enterococcal strains producing mutant forms of PrgB, e.g., with missing or defective aggregation domains, displayed highly attenuated colonization compared with a plasmid-free strain. To account for these findings, it was postulated that elaboration of such PrgB mutant proteins around the cell surface could simultaneously block formation of cell-cell contacts necessary for recruitment of planktonic cells to sites of initial colonization and also physically mask presentation of other surface adhesins or virulence factors that could functionally substitute for PrgB (Chuang *et al.* 2009, Chuang-Smith *et al.*, 2010). The Δ*prgA* or Δ*prgC* mutations might phenocopy the *prgB* domain mutations by simultaneously interfering with assembly of functional Prg adhesin complexes and masking presentation of alternative chromosomal adhesins or virulence factors. Whether PrgA and PrgC act directly or indirectly to promote colonization and infection remains to be determined using both invertebrate and mammalian infection models.

In summary, we have shown that the pCF10-encoded Prg surface factors significantly enhance the efficiency with which plasmid-carrying cells develop biofilms and enhance virulence using the worm model. We propose that PrgA and PrgB, and possibly also PrgC, interact to form a fibrous mesh that coats the *E. faecalis* cell surface and serves as a stratum for recruitment of ECM components (eDNA, LTA, EPS) secreted or released by autolysis. Binding of these matrix components by viable donor cells plays a critical role in cell-cell aggregation and attachment to surfaces. Previously, it was shown that mixed populations of induced pCF10-carrying donors and plasmid-free recipients form robust aggregates even when 90% or more of the population are recipients (Olmsted *et al.*, 1991). In nature, the DNA-containing extracellular matrix resulting from pheromone induction likely plays an important role in recruitment and concentration of plasmid-bearing and -free enterococci, as well as other species, during establishment of dense biofilm communities. In such settings, Prg-mediated biofilm development would ensure the efficient transfer of pCF10 or related pheromone-dependent plasmids among *E. faecalis*, as well as the mobilization of other plasmids or chromosomal fragments bearing selective traits, e.g., antibiotic resistance genes or virulence determinants (Manson *et al*., 2010), to other medically-important species.

EXPERIMENTAL PROCEDURES

Bacterial strains and growth conditions

The plasmids directly used in this study are listed in Table 1, and a complete list of bacterial strains, plasmids, and oligonucleotides is presented in the Supplementary Table. *E. coli* DH5α and EC1000, a strain that produces the pWV01 RepA protein (Leenhouts *et al.*, 1996), were used as hosts for plasmid constructions. *E. coli* strains were grown in Luria broth (LB; Difco Laboratories) or brain heart infusion broth (BHI; Difco Laboratories) at 37°C with shaking. The following antibiotics were added to *E. coli* cultures as needed: chloramphenicol (20 μg ml^{-1}), erythromycin (100 μg ml^{-1}), spectinomycin (50 μg ml^{-1}), gentamycin (10 μg ml^{-1}) and kanamycin (50 μg ml^{-1}). *E. faecalis* OG1RF and OG1ES served as plasmid donor and recipient strains in the mating assays respectively, and OG1RF or chromosomal variants served as hosts for all other experiments. *E. faecalis* strains were

grown in BHI or tryptic soy broth (TSB; Difco Laboratories) at 37°C without shaking. The following antibiotics were added to *E. faecalis* cultures as needed: erythromycin (100 μg ml^{-1} for plasmid-encoded resistance genes, 10 μg ml^{-1} for chromosomal-encoded genes), fusidic acid (25 μg ml^{-1}), rifampin (200 μg ml^{-1}), spectinomycin (1,000 μg $ml^{-1}$for plasmid-encoded genes, 250 μg $ml^{-1}$for chromosomal-encoded genes), streptomycin (1,000 μg ml^{-1}), tetracycline (10 μg ml^{-1}), and chloramphenicol (10 μg ml^{-1}). All antibiotics were obtained from Sigma Chemical Co.

Construction of prgA and prgC in-frame deletion mutations

For the construction of pCF10Δ*prgA* and pCF10Δ*prgC*, ~500-600 base-pair (bp) regions immediately upstream of each gene were amplified with forward and reverse (F/R) primers designated prgAup or prgCup. Fragments of similar size immediately downstream of both genes were amplified using the prgAdown or prgCdown F/R primers. The fragments were joined by overlapping PCR, and the resulting constructs were introduced into pCJK47 (Suppl. Table) using the primer-added XbaI/NcoI restriction sites, resulting in pMCM1 and pMCM2 respectively. These plasmids were used to delete *prgA* and *prgC* from pCF10 or pCF10Δ*oriT* by marker-less exchange recombination (Kristich *et al.*, 2007) to obtain plasmids pCF10Δ*prgA* and pCF10Δ*prgC*, respectively. Plasmid pCF10Δ*prgA-C* was constructed as follows. The prgAdown fragment was removed from pMCM1 by digestion with XmaI/NcoI, and substituted with the corresponding prgCdown fragment isolated by XmaI/NcoI digestion from pMCM2. The resulting plasmid, pMB1, was used for deletion of the entire *prgA* through *prgC* region from pCF10 using marker-less exchange recombination (Kristich *et al.*, 2007).

prgA, prgB, and prgC expression plasmids

prgA, prgB and *prgC* were cloned downstream of a constitutive *Lactococcus lactis* promoter P_{23} (Chen *et al.*, 2007) resulting in plasmids pMB2, pMB3 and pMB4, respectively. For these constructions, *prgA* and *prgB* were amplified using pCF10 as a template and gene specific F and R primers with BamHI and SphI restriction sites, respectively. *prgC* was amplified using F and R primers with SalI and SphI restriction sites, respectively. PCR products were digested using the specified restriction enzymes and introduced into similarly digested pDLP278p23 (Chen *et al.*, 2007). The amplified *prgA, prgB*, and *prgC* genes were also introduced into the plasmid pCIE (Y. Chen and G. Dunny, unpublished), which carries the entire *prgQ* regulatory region for pheromone-inducible expression of cloned genes from the native pCF10 promoter, resulting in plasmids pMB5, pMB6 and pMB7, respectively. All *prg* expression plasmids were introduced into *E. faecalis* strain OG1RF carrying pCF10 variants by electroporation (Dunny *et al.*, 1991).

Conjugation assays

Single colonies of *E. faecalis* donor strains (OG1RF background) and the recipient strain (OG1ES) were inoculated in BHI and grown overnight without shaking. Cultures were then diluted 1:10 in BHI and grown for 1 h at 37°C without shaking. The donor and recipient strains were mixed in a ratio of 1:10. The strains were allowed to mate in liquid without shaking, and 10 μl of the mating mix was also spotted onto nitrocellulose placed on BHI

plates. We also assessed the effects of vigorous shaking of liquid mating mixtures on plasmid transfer frequencies. To evaluate the effect of DNase on conjugative transfer, 2 U μl^{-1} of DNase I (Roche) was added at the onset of mating. After 2 h of mating, the filters were re-suspended in 1ml of 1X PBS. Mating mixtures from the liquid and solid-surface matings were serially diluted in 1X PBS, and the numbers of donors and transconjugants were obtained by plating on selective BHI agar plates. The plasmid transfer frequencies were calculated as the number of transconjugants per donor cell (Chen *et al.*, 2008). The results reported are an average of at least three different experiments.

Prg *or* Pcf *protein detection by immunoblotting*

Exponential-phase cultures (5 ml) of *E. facealis* strains carrying pCF10 or pCF10 variants normalized to an OD_{600} of 0.3 were induced with 10 ng ml^{-1} of peptide cCF10 for 1 h at 37 °C. The cells were pelleted by centrifugation at 13,200 × *g* for 15 min at 4 °C and washed once with cold 1X physiological buffer saline (PBS). The pellet was resuspended in 125 μl of SMM buffer (0.5M sucrose, 0.02M $MgCl_2$, 0.02M maleate, pH 6.5) containing 60 μl ml^{-1} of mutanolysin (Sigma-Aldrich) and 10 mg ml^{-1} of lysozyme (Sigma-Aldrich), then incubated for 1 h at 37 °C with shaking. Material released from the digested cell wall was separated from cell-bound material by centrifugation at 13,200 *x g* for 15 min at 4 °C (Chang *et al.*, 2013). Equal amounts of the cell-wall (supernatant) and cell-bound (pellet) fractions were electrophoresed through sodium dodecyl sulfate (SDS)-polyacrylamide gels, and the surface proteins PrgA, PrgB, or PrgC or the T4SS machine subunits PrgJ, PcfC or PcfG were detected by Western transfer and immunostaining with the appropriate antibodies (Christie *et al.*, 1988, Chen *et al.*, 2007, Chen *et al.*, 2008, Li*et al.*, 2012).

RT-qPCR

Three colonies of each strain were inoculated into 10 ml M9-YE (Dunny and Clewell, 1975) and incubated at 37°C for 14.5 -16 h. Cultures were diluted 1:10 into 10 ml fresh M9-YE, further incubated for 1 h, and then induced with 5 ng/ml cCF10. Aliquots of cells collected at 0, 30, and 60 min post-induction were treated with RNAprotect Bacteria Reagent (Qiagen, Inc., Valencia, CA) according to the manufacturer's instructions. Cell pellets were resuspended in TE (10 mM Tris-HCl pH 8, 1 mM EDTA) containing 500 U/ml mutanolysin and 30 mg/ml lysozyme and incubated at 37°C for 10 min. RNA was extracted with the RNeasy Mini Kit (Qiagen, Inc.) according to the manufacturer's instructions. Contaminating DNA was removed with the Turbo-DNA free kit (Ambion). cDNA was synthesized with random hexamers using the Superscript III First-Strand Synthesis System (Invitrogen Corp.) according to the manufacturer's instructions. Quantitative PCR was carried out as previously described (Frank *et al.*, 2012). *gyrB* was used as a reference gene. Two biological replicates were performed with similar results.

DNase and aggregation assays

Overnight cultures of *E. faecalis* strains were diluted 1:10 in fresh BHI and grown at 37°C for 1 h. This culture was further diluted 1:100 with BHI containing 10 ng ml^{-1} of the peptide cCF10; 2U μl^{-1} of DNase I was added to one set of cultures. The effect of DNase treatment

on cCF10-induced aggregation was monitored over time using a Klett meter and by visual inspection.

Biofilm assays

Biofilm formation was evaluated with a crystal violet plate assay and by fluorescence microscopy. The plate biofilm assay was performed as described by Mohamed et al (Mohamed *et al.*, 2004) with modifications. Briefly, overnight cultures of strains were diluted 1:100 in 200 µl of TSB containing 0.25% of glucose and 10 ng ml^{-1} of cCF10 with or without 2U $µl^{-1}$ of DNase I in a 96-well polystyrene flat-bottomed microtiter plate (Greiner Bio-One) and incubated for 24 h at 37 °C under static conditions. At least six wells were inoculated per strains. The wells were washed 3 times with 1 X PBS to remove the non-adherent cells. The plates were dried at 60 °C for 1 h and then stained with 0.1% crystal violet (CV) for 15 min at room temperature. The wells were washed 3 times with 1 X PBS to remove unbound CV. Ethanol was used to solubilize CV after which the optical density (OD) was measured at 540 nm. The results describe the average percentage reduction of biomass relative to pCF10 for 3 independent experiments. The *P* values were calculated by analysis of variance followed by Newman Keul post hoc test to identify difference between group means using GraphPad Prism (version 5.0). *P* values of <0.05 were considered statistically significant.

For microscopic visualization of the biofilms, logarithmic-phase cultures of the strains were diluted 1:100 in TSB containing 0.25% of glucose and 10 ng ml^{-1} of cCF10 in a 24 well tissue culture plate (Becton-Dickson) containing four polymethylmethacrylate (PMMA) 5 mm diameter coupons. The coupons were pre-incubated with the media overnight at 4 °C. For each strain, four coupons were used and each experiment was repeated at least twice. The plate containing the coupons was incubated at 37 °C under static conditions for specific time periods, and media in each well was changed after 24 h. Each coupon was stained for 15 min with 1 ml of 1X PBS containing 10 µl of 1 % calcofluor white and 1.5 µl of 0.5 % hexidium iodide (HI) in DMSO. For eDNA visualization, the coupons were first stained in 1 ml of 1X PBS containing 1µl of 1X GelGreen (Biotium) for 5 min followed by calcofluor white and HI staining as described above (Tribble et al., 2012). After staining, the coupons were visualized using an Olympus IX 81 fluorescence microscope. The 3-D images were collected at 40X magnification and compiled using Slidebook software (version 6). Images presented in Figs. 5 and 6 correspond to a slice in the center of the biofilm. The thickness of each biofilm was determined as the number of 1 µM slices collected. The total fluorescence intensity (FI) for each channel of the biofilm images was calculated as the sum of FI's for all collected slices using Slidebook software. The values presented in Table S1 are a percentage of the value for OR1RF(pCF10) biofilms.

eDNA quantitation

Overnight cultures of strains were diluted 1:100 in a total of 15 ml of TSB containing 0.25% of glucose and 10 ng ml^{-1} of cCF10. Cultures were inoculated onto polystyrene petri plates and incubated at 37 °C without shaking for 8 and 24 h. The supernatant was removed and biofilm cells were resuspended in 750 µl of 50 mM EDTA and treated with proteinase K. Cells were pelleted by centrifugation for CFU determinations, and eDNA in the remaining

supernatant was recovered by ethanol precipitation. eDNA was electrophoresed through agarose gels and stained with ethidium bromide to visualize high molecular weight DNA (Thomas *et al.*, 2008). eDNA was quantitated by densitometric spot comparisons using alphaimager software (Alpha-Innotec, CA) and relative levels were reported in arbitrary units per CFU.

C. elegans killing assay

The *C. elegans* killing assay was performed as previously described (Garsin *et al.*, 2001). Briefly, a single colony of each *E. faecalis* strain was used to inoculate 2 ml of BHI. After growing the cells at 37 °C for 4 - 5 h, 10 μl of the culture was spread on BHI agar in a 35-mm tissue-culture plates. Gentamycin (10 μg/ml) was added to the medium to selectively prevent growth of *E. coli*. *C. elegans* strain N2 was maintained and propagated on *E. coli* strain OP50 with standard techniques (Garsin *et al.*, 2001, Sifri *et al.*, 2002). Between 20 and 30 *C. elegans* L4 or young adult hermaphrodites were transferred from a lawn of *E. coli* OP50 to a lawn of the bacterium to be tested, incubated at 25°C, and examined at ~24-h intervals with a dissecting microscope for viability. Worms were considered dead when they did not respond to a platinum wire pick. Each experiment was repeated at least three times. *C. elegans* survival was plotted with the Kaplan–Meier method using GraphPad Prism (version 5.0). *P* values of <0.05 were considered statistically significant. Bacterial counts from *C. elegans* infected with *E. faecalis* strains were performed after 1, 3 and 5 days of infection as previously described (Garsin et al., 2001). The results represent the average of the triplicate samples evaluated at each time.

Supplementary Material

Refer to Web version on PubMed Central for supplementary material.

ACKNOWLEDGEMENTS

We thank Dr. Barbara Murray for providing strains used in the study and Maria Camilla Montealegre for help with strain and plasmid constructions. We thank members of our respective laboratories for helpful discussions. These studies were supported by NIH grants R01GM48746 (P.J.C), R21AI105454 (P.J.C & G.M.D), R01GM49530 (G.M.D), R01AI076406 and R56AI110432 (D.A.G), and R01DE021394 (H.B.K.).

REFERENCES

Alvarez-Martinez CE, Christie PJ. Biological diversity of prokaryotic type IV secretion systems. Microbiol Mol Biol Rev. 2009; 73:775–808. [PubMed: 19946141]

Banin R, Brady KM, Greenberg EP. Chelator-induced dispersal and killing of *Pseudomonas aeruginosa* cells in a biofilm. Appl Environ Microbiol. 2006; 72:2064–2069. [PubMed: 16517655]

Barnes AM, Ballering KS, Leibman RS, Wells CL, Dunny GM. *Enterococcus faecalis* produces abundant extracellular structures containing DNA in the absence of cell lysis during early biofilm formation. MBio. 2012; 3:e00193–00112. [PubMed: 22829679]

Bhatty M, Laverde Gomez JA, Christie PJ. The expanding bacterial type IV secretion lexicon. Res Microbiol. 2013; 164:620–639. [PubMed: 23542405]

Cavaliere R, Ball JL, Turnbull L, Whitchurch CB. The biofilm matrix destabilizers, EDTA and DNaseI, enhance the susceptibility of nontypeable Hemophilus influenzae biofilms to treatment with ampicillin and ciprofloxacin. Microbiologyopen. 2014; 3:557–5676. [PubMed: 25044339]

Chang C, Huang IH, Hendrickx AP, Ton-That H. Visualization of Gram-positive bacterial pili. Methods Mol Biol. 2013; 966:77–95. [PubMed: 23299729]

Chatterjee A, Cook LC, Shu CC, Chen Y, Manias DA, Ramkrishna D, et al. Antagonistic self-sensing and mate-sensing signaling controls antibiotic-resistance transfer. Proc Natl Acad Sci U S A. 2013; 110:7086–7090. [PubMed: 23569272]

Chen Y, Staddon JH, Dunny GM. Specificity determinants of conjugative DNA processing in the *Enterococcus faecalis* plasmid pCF10 and the *Lactococcus lactis* plasmid pRS01. Mol Microbiol. 2007; 63:1549–1564. [PubMed: 17302827]

Chen Y, Zhang X, Manias D, Yeo HJ, Dunny GM, Christie PJ. *Enterococcus faecalis* PcfC, a spatially localized substrate receptor for type IV secretion of the pCF10 transfer intermediate. J Bacteriol. 2008; 190:3632–3645. [PubMed: 18326569]

Christie PJ, Dunny GM. Identification of regions of the *Streptococcus faecalis* plasmid pCF-10 that encode antibiotic resistance and pheromone response functions. Plasmid. 1986; 15:230–241. [PubMed: 3012615]

Christie PJ, Kao SM, Adsit JC, Dunny GM. Cloning and expression of genes encoding pheromone-inducible antigens of *Enterococcus (Streptococcus) faecalis*. J Bacteriol. 1988; 170:5161–5168. [PubMed: 2846512]

Chuang ON, Schlievert PM, Wells CL, Manias DA, Tripp TJ, Dunny GM. Multiple functional domains of *Enterococcus faecalis* aggregation substance Asc10 contribute to endocarditis virulence. Infect Immun. 2009; 77:539–548. [PubMed: 18955479]

Chuang-Smith ON, Wells CL, Henry-Stanley MJ, Dunny GM. Acceleration of *Enterococcus faecalis biofilm* formation by aggregation substance expression in an *ex vivo* model of cardiac valve colonization. PLoS ONE. 2010; 5:e15798. [PubMed: 21209892]

Cook LC, Chatterjee A, Barnes A, Yarwood J, Hu W-S, Dunny GM. Biofilm growth alters regulation of conjugation by a bacterial pheromone. Mol Microbiol. 2011; 81:1499–1510. [PubMed: 21843206]

Cook LC, Dunny GM. Effects of biofilm growth on plasmid copy number and expression of antibiotic resistance genes in *Enterococcus faecalis*. Antimicrob Agents Chemother. 2013; 57:1850–1856. [PubMed: 23380728]

Das T, Sehar S, Koop L, Wong YK, Ahmed S, Siddiqui KS, Manefield M. Influence of calcium in extracellular DNA mediated bacterial aggregation and biofilm formation. PLoS One. 2014; 9:e91935. [PubMed: 24651318]

Dunny G, Funk C, Adsit J. Direct stimulation of the transfer of antibiotic resistance by sex pheromones in *Streptococcus faecalis*. Plasmid. 1981; 6:270–278. [PubMed: 6796985]

Dunny GM. Enterococcal sex pheromones: signaling, social behavior, and evolution. Annu Rev Genet. 2013; 47:457–482. [PubMed: 24050179]

Dunny GM, Brown BL, Clewell DB. Induced cell aggregation and mating in *Streptococcus faecalis*: evidence for a bacterial sex pheromone. Proc Natl Acad Sci U S A. 1978; 75:3479–3483. [PubMed: 98769]

Dunny GM, Clewell DB. Transmissible toxin (hemolysin) plasmid in *Streptococcus faecalis* and its mobilization of a noninfectious drug resistance plasmid. J Bacteriol. 1975; 124:784–790. [PubMed: 810482]

Dunny, GM.; Hancock, LE.; Shankar, N. Enterococcal biofilm structure and role in colonization and disease.. In: Gilmore, MS.; Clewell, DB.; Ike, Y.; Shankar, N., editors. Enterococci: From commensals to leading causes of drug resistant infection [Internet]. Massachusetts Eye and Ear Infirmary; Boston: 2014. http://www.ncbi.nlm.nih.gov/books/NBK190433/

Dunny GM, Lee LN, LeBlanc DJ. Improved electroporation and cloning vector system for Gram-positive bacteria. Appl Environ Microbiol. 1991; 57:1194–1201. [PubMed: 1905518]

Dunny GM, Zimmerman DL, Tortorello ML. Induction of surface exclusion (entry exclusion) by *Streptococcus faecalis* sex pheromones: use of monoclonal antibodies to identify an inducible surface antigen involved in the exclusion process. Proc Natl Acad Sci U S A. 1985; 82:8582–8586. [PubMed: 3936037]

Flemming HC, Wingender J. The biofilm matrix. Nat Rev Microbiol. 2010; 8:623–633. [PubMed: 20676145]

Frank KL, Barnes AM, Grindle SM, Manias DA, Schlievert PM, Dunny GM. Use of recombinase-based *in vivo* expression technology to characterize *Enterococcus faecalis* gene expression during infection identifies in vivo-expressed antisense RNAs and implicates the protease Eep in pathogenesis. Infect Immun. 2012; 80:539–549. [PubMed: 22144481]

Garsin, DA.; Frank, KL.; Silanpaa, J.; Ausubel, FM.; Hartke, A.; Shankar, N.; Murray, BE. Pathogenesis and models of enterococcal infection.. In: Gilmore, MS.; Clewell, DB.; Ike, Y.; Shankar, N., editors. Enterococci: From commensals to leading causes of drug resistant infection. Massachusetts Eye and Ear Infirmary; Boston: 2014. http://www.ncbi.nlm.nih.gov/books/NBK190424/

Garsin DA, Sifri CD, Mylonakis E, Qin X, Singh KV, Murray BE, et al. A simple model host for identifying Gram-positive virulence factors. Proc Natl Acad Sci U S A. 2001; 98:10892–10897. [PubMed: 11535834]

Hirt H, Erlandsen SL, Dunny GM. Heterologous inducible expression of *Enterococcus faecalis* pCF10 aggregation substance Asc10 in *Lactococcus lactis* and *Streptococcus gordonii* contributes to cell hydrophobicity and adhesion to fibrin. J Bacteriol. 2000; 182:2299–2306. [PubMed: 10735875]

Hirt H, Manias DA, Bryan EM, Klein JR, Marklund JK, Staddon JH, et al. Characterization of the pheromone response of the *Enterococcus faecalis* conjugative plasmid pCF10: complete sequence and comparative analysis of the transcriptional and phenotypic responses of pCF10-containing cells to pheromone induction. J Bacteriol. 2005; 187:1044–1054. [PubMed: 15659682]

Kelley LA, Sternberg MJ. Protein structure prediction on the Web: a case study using the Phyre server. Nat Protoc. 2009; 4:363–371. [PubMed: 19247286]

Kristich CJ, Chandler JR, Dunny GM. Development of a host-genotype-independent counterselectable marker and a high-frequency conjugative delivery system and their use in genetic analysis of *Enterococcus faecalis*. Plasmid. 2007; 57:131–144. [PubMed: 16996131]

Leenhouts K, Buist G, Bolhuis A, ten Berge A, Kiel J, Mierau I, et al. A general system for generating unlabelled gene replacements in bacterial chromosomes. Mol Gen Genet. 1996; 253:217–224. [PubMed: 9003306]

Li F, Alvarez-Martinez C, Chen Y, Choi KJ, Yeo HJ, Christie PJ. *Enterococcus faecalis* PrgJ, a VirB4-like ATPase, mediates pCF10 conjugative transfer through substrate binding. J Bacteriol. 2012; 194:4041–51. [PubMed: 22636769]

Liu HH, Yang YR, Shen XC, Zhang ZL, Shen P, Xie ZX. Role of DNA in bacterial aggregation. Curr Microbiol. 2008; 57:139–144. [PubMed: 18491189]

Lovdok L, Bentele K, Vladimirov N, Muller A, Pop FS, Lebiedz D, et al. Role of translational coupling in robustness of bacterial chemotaxis pathway. PLoS Biology. 2009; 7:e1000171. [PubMed: 19688030]

Manson JM, Hancock LE, Gilmore MS. Mechanism of chromosomal transfer of *Enterococcus faecalis* pathogenicity island, capsule, antimicrobial resistance, and other traits. Proc Nat Acad Sci USA. 2010; 107:12269–12274. [PubMed: 20566881]

Mohamed JA, Huang W, Nallapareddy SR, Teng F, Murray BE. Influence of origin of isolates, especially endocarditis isolates, and various genes on biofilm formation by *Enterococcus faecalis*. Infect Immun. 2004; 72:3658–3663. [PubMed: 15155680]

Navarre WW, Schneewind O. Surface proteins of gram-positive bacteria and mechanisms of their targeting to the cell wall envelope. Microbiol Mol Biol Rev. 1999; 63:174–229. [PubMed: 10066836]

O'Toole GA, Kolter R. Initiation of biofilm formation in *Pseudomonas fluorescens* WCS365 proceeds via multiple, convergent signalling pathways: a genetic analysis. Mol Microbiol. 1998; 28:449–461. [PubMed: 9632250]

Oli MW, Otoo HN, Crowley PJ, Heim KP, Nascimento MM, Ramsook CB, et al. Functional amyloid formation by *Streptococcus mutans*. Microbiology. 2012; 158:2903–2916. [PubMed: 23082034]

Olmsted SB, Erlandsen SL, Dunny GM, Wells CL. High-resolution visualization by field emission scanning electron microscopy of *Enterococcus faecalis* surface proteins encoded by the pheromone-inducible conjugative plasmid pCF10. J Bacteriol. 1993; 175:6229–6237. [PubMed: 8407795]

Olmsted SB, Kao SM, van Putte LJ, Gallo JC, Dunny GM. Role of the pheromone-inducible surface protein Asc10 in mating aggregate formation and conjugal transfer of the *Enterococcus faecalis* plasmid pCF10. J Bacteriol. 1991; 173:7665–7672. [PubMed: 1938962]

Qin X, Singh KV, Weinstock GM, Murray BE. Characterization of *fsr*, a regulator controlling expression of gelatinase and serine protease in *Enterococcus faecalis* OG1RF. J Bacteriol. 2001; 183:3372–3382. [PubMed: 11344145]

Rakita RM, Vanek NN, Jacques-Palaz K, Mee M, Mariscalco MM, Dunny GM, et al. *Enterococcus faecalis* bearing aggregation substance is resistant to killing by human neutrophils despite phagocytosis and neutrophil activation. Infect Immun. 1999; 67:6067–6075. [PubMed: 10531268]

Rice KC, Mann EE, Endres JL, Weiss EC, Cassat JE, Smeltzer MS, Bayles KW. The *cidA* murein hydrolase regulator contributes to DNA release and biofilm development in *Staphylococcus aureus*. Proc Natl Acad Sci U S A. 2007; 104:8113–8118. [PubMed: 17452642]

Schlievert PM, Chuang-Smith ON, Peterson ML, Cook LC, Dunny GM. *Enterococcus faecalis* endocarditis severity in rabbits is reduced by IgG Fabs interfering with aggregation substance. PLoS ONE. 2010; 5:e13194. [PubMed: 20957231]

Schlievert PM, Gahr PJ, Assimacopoulos AP, Dinges MM, Stoehr JA, Harmala JW, et al. Aggregation and binding substances enhance pathogenicity in rabbit models of *Enterococcus faecalis* endocarditis. Infect Immun. 1998; 66:218–223. [PubMed: 9423861]

Sifri CD, Mylonakis E, Singh KV, Qin X, Garsin DA, Murray BE, et al. Virulence effect of *Enterococcus faecalis* protease genes and the quorum-sensing locus *fsr* in *Caenorhabditis elegans* and mice. Infect Immun. 2002; 70:5647–5650. [PubMed: 12228293]

Singh KV, Nallapareddy SR, Sillanpaa J, Murray BE. Importance of the collagen adhesin Ace in pathogenesis and protection against *Enterococcus faecalis* experimental endocarditis. PLoS Pathog. 2010; 6:e1000716. [PubMed: 20072611]

Staddon JH, Bryan EM, Manias DA, Chen Y, Dunny GM. Genetic characterization of the conjugative DNA processing system of enterococcal plasmid pCF10. Plasmid. 2006; 56:102–111. [PubMed: 16774784]

Sussmuth SD, Muscholl-Silberhorn A, Wirth R, Susa M, Marre R, Rozdzinski E. Aggregation substance promotes adherence, phagocytosis, and intracellular survival of *Enterococcus faecalis* within human macrophages and suppresses respiratory burst. Infect Immun. 2000; 68:4900–4906. [PubMed: 10948103]

Thomas VC, Thurlow LR, Boyle D, Hancock LE. Regulation of autolysis-dependent extracellular DNA release by *Enterococcus faecalis* extracellular proteases influences biofilm development. J Bacteriol. 2008; 190:5690–5698. [PubMed: 18556793]

Tribble GD, Rigney TW, Dao DH, Wong CT, Kerr JE, Taylor BE, et al. Natural competence is a major mechanism for horizontal DNA transfer in the oral pathogen *Porphyromonas gingivalis*. MBio. 2012; 3:e00231–11. [PubMed: 22294679]

Wastfelt M, Stalhammar-Carlemalm M, Delisse AM, Cabezon T, Lindahl G. Identification of a family of streptococcal surface proteins with extremely repetitive structure. J Biol Chem. 1996; 271:18892–18897. [PubMed: 8702550]

Waters CM, Dunny GM. Analysis of functional domains of the *Enterococcus faecalis* pheromone-induced surface protein aggregation substance. J Bacteriol. 2001; 183:5659–5667. [PubMed: 11544229]

Waters CM, Hirt H, McCormick JK, Schlievert PM, Wells CL, Dunny GM. An amino-terminal domain of *Enterococcus faecalis* aggregation substance is required for aggregation, bacterial internalization by epithelial cells and binding to lipoteichoic acid. Mol Microbiol. 2004; 52:1159–1171. [PubMed: 15130132]

Whitchurch CB, Tolker-Nielsen T, Ragas PC, Mattick JS. Extracellular DNA required for bacterial biofilm formation. Science. 2002; 295:1487. [PubMed: 11859186]

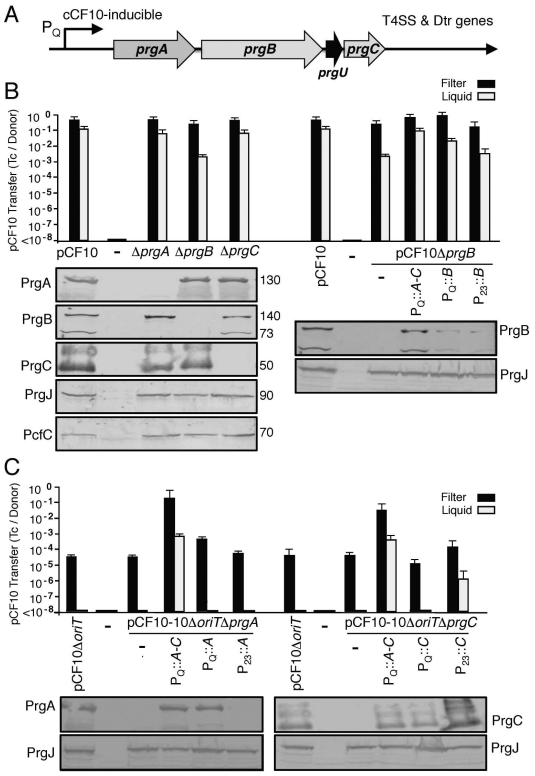

FIG. 1. Individual *prg* genes enhance but are not required for pCF10 transfer

(A) Schematic representation of the pCF10 *prg* gene cluster encoding PrgA (891 residues), PrgB (1,305 residues), PrgU (118 residues), PrgC (285 residues) relative to the pheromone-inducible P_Q promoter and downstream T4SS and Dtr processing genes. **(B)** Histogram: Transfer frequencies of pCF10 plasmids in 2 h filter and liquid matings. Donor strains: OG1RF lacking (−) or carrying pCF10 or pCF10Δ*prg* mutant plasmids (left), or pCF10Δ*prgB* and complementing plasmids expressing the *prg* genes (right). Complementing plasmids: P_Q::*prgA-C* (pINY1801), P_Q::*prgB* (pMB6), P_{23}::*prgB* (pMB3). Transfer frequencies are presented as the number of transconjugants per donor cell (Tc's/ Donor). Experiments were repeated at least 3 times and the histogram depicts the average values with standard deviations. Immunoblots: Steady state levels of PrgA, PrgB, PrgC,PrgJ and PcfC in *E. faecalis* OG1RF strains lacking (-) or carrying the pCF10 variants and *prg* expression constructs listed above each lane. The immunoblots were developed with antibodies to the proteins listed and the approximate size of the detected protein in kilodaltons (kDa's) is listed at the right. Protein extracts were loaded on a per-cell equivalent basis. **(C)** Histogram: Transfer frequencies in 2 h filter and liquid matings with OG1RF donors carrying pCF10Δ*oriT*, pCF10Δ*oriT*Δ*prgA*, or pCF10Δ*oriT*Δ*prgC* and complementing plasmids expressing the genes listed. Complementing plasmids: P_Q::*prgA-C* (pINY1801), P_Q::*prgA* (pMB5), P_{23}::*prgA* (pMB2), P_Q::*prgC* (pMB7), P_{23}::*prgC* (pMB4). Immunoblots: Steady-state levels of PrgA, PrgC, or PrgJ in the strains listed above each lane as detected by Western immunoblotting.

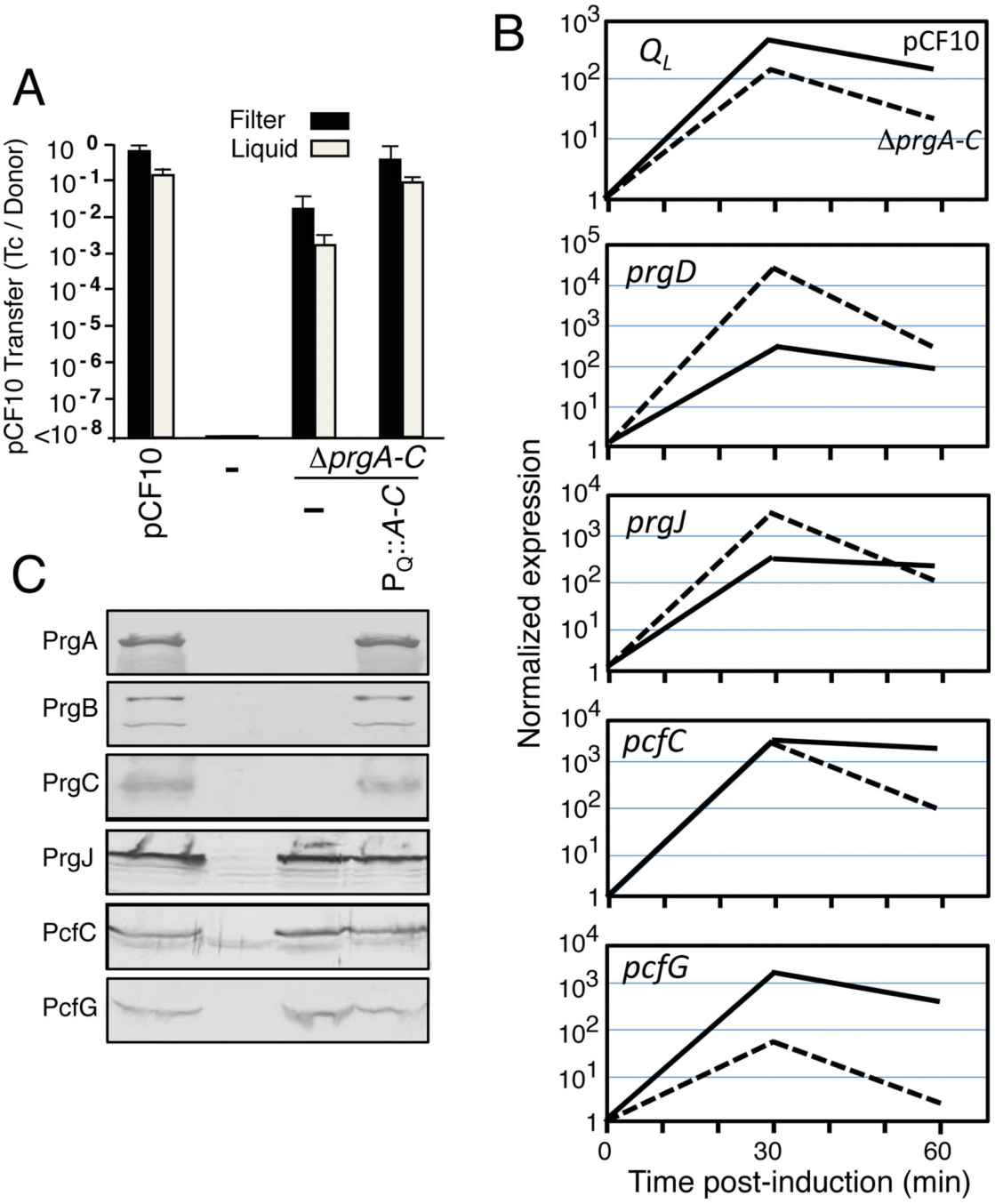

FIG. 2. Deletion of the entire *prgA-C* gene cluster only modestly diminishes plasmid transfer

(A) Transfer frequencies of OG1RF strains lacking or carrying pCF10, pCF10Δ*prgA-C* alone or with the P_Q::*prgA-C* expression plasmid pINY1801 in 2 h filter and liquid matings. Transfer frequencies are presented as the number of transconjugants per donor cell (Tc's/Donor). Experiments were repeated at least 3 times and the histogram depicts average values with standard deviations. **(B)** qRT-PCR results showing the relative expression levels of regions of the *prgQ* operon located upstream (Q_L) and downstream (*prgD, prgJ, pcfC, pcfG*) of the *prgA-C* genes in pCF10 (solid lines) and pCF10Δ*prgA-C* (dashed lines) at 30 and 60

min following cCF10 pheromone induction with 5ng/ml cCF10. The data shown are from one biological replicate, which was repeated with similar results. **(C)** Steady state levels of pCF10-encoded surface proteins (PrgA, PrgB, PrgC) and downstream T4SS machine subunits (PrgJ, PcfC, PcfG) in *E. faecalis* OG1RF without (−) and with pCF10; pCF10Δ*prgA-C* or pCF10Δ*prgA-C* and the P_Q::*prgA-C* expression plasmid pINY1801. Immunoblots were developed with antibodies to the proteins listed on the left. Protein extracts were loaded on a per-cell equivalent basis.

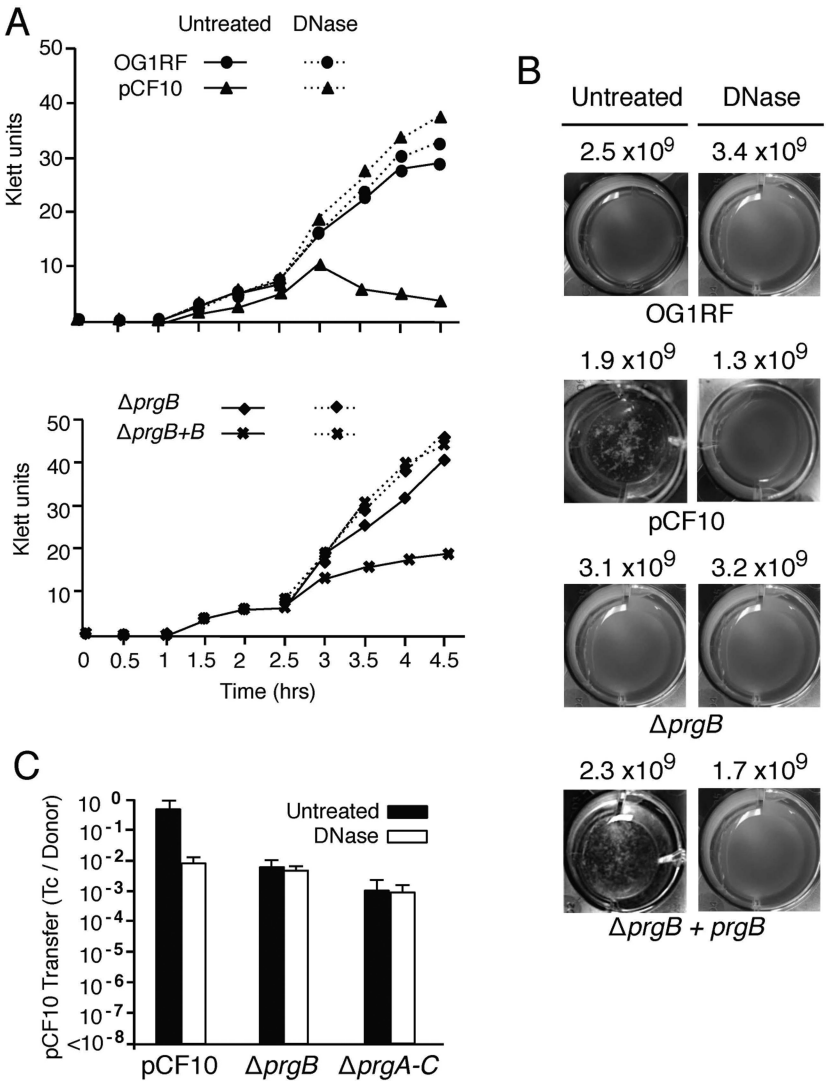

FIG. 3. PrgB-mediated aggregation and plasmid transfer is dependent on eDNA

(A) Aggregation assays showing the effects of DNase treatment on pheromone (cCF10)-induced cellular aggregation. DNase treatment inhibited aggregation of OG1RF(pCF10) (upper graph) and OG1RF(pCF10Δ*prgB*, pMB6) expressing P_Q::*prgB* (lower graph). **(B)** Photographs of cells grown in microtiter plates showing the effects of DNase on pheromone-induced clumping at 14 h following pheromone induction. Strains: OG1RF lacking or carrying pCF10, pCF10Δ*prgB*, or pCF10Δ*prgB* and pMB6. The numbers correspond to colony forming units (CFU's) per ml at 14 h following cCF10 induction in absence (Untreated) or presence of DNase. **(C)** Histograms depict the transfer frequencies of pCF10, pCF10Δ*prgB* and pCF10Δ*prgA-C* without or with DNase added at the onset of a 2 h liquid mating.

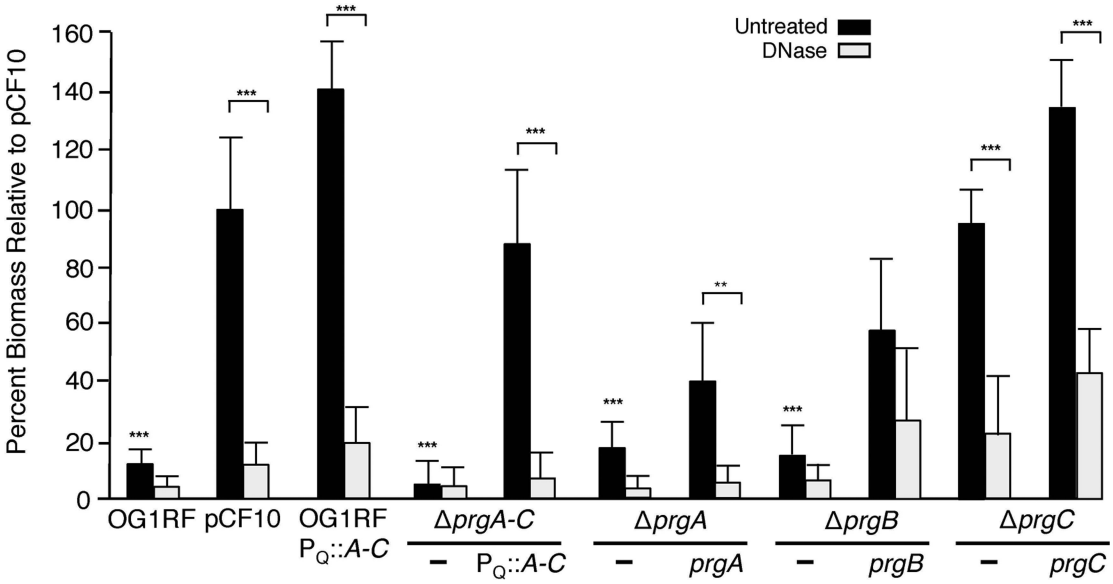

FIG. 4. PrgA and PrgB mediate DNase-sensitive adherence to polystyrene

Biofilm formation by *prg* mutant strains on polystyrene microtiter plates. Strains: OG1RF, OG1RF(pCF10), or OG1RF strains carrying Δ*prg* mutant plasmids and complementing plasmids are shown. Complementing plasmids: P_Q::*prgA* (pMB5), P_Q::*prgB* (pMB6), P_Q::*prgC* (pMB7), and P_Q::*prgA-C* (pINY1801). The biofilm biomass was assayed as a function of crystal violet stain retained. DNase treatment was initiated at the onset of cCF10 induction and biofilm formation and continued for the full incubation time of 24 h. Results are expressed as the percentage biomass relative to pCF10 and represent the average of at least three independent experiments; the error bars represent standard deviation. Statistically significant differences (***P<0.001; **P<0.01) were evaluated within each strain with respect to DNase treatment (brackets) and across the untreated group with respect to strains containing pCF10 (no brackets) using one-way analysis of variance followed by Newman-Keuls post hoc test.

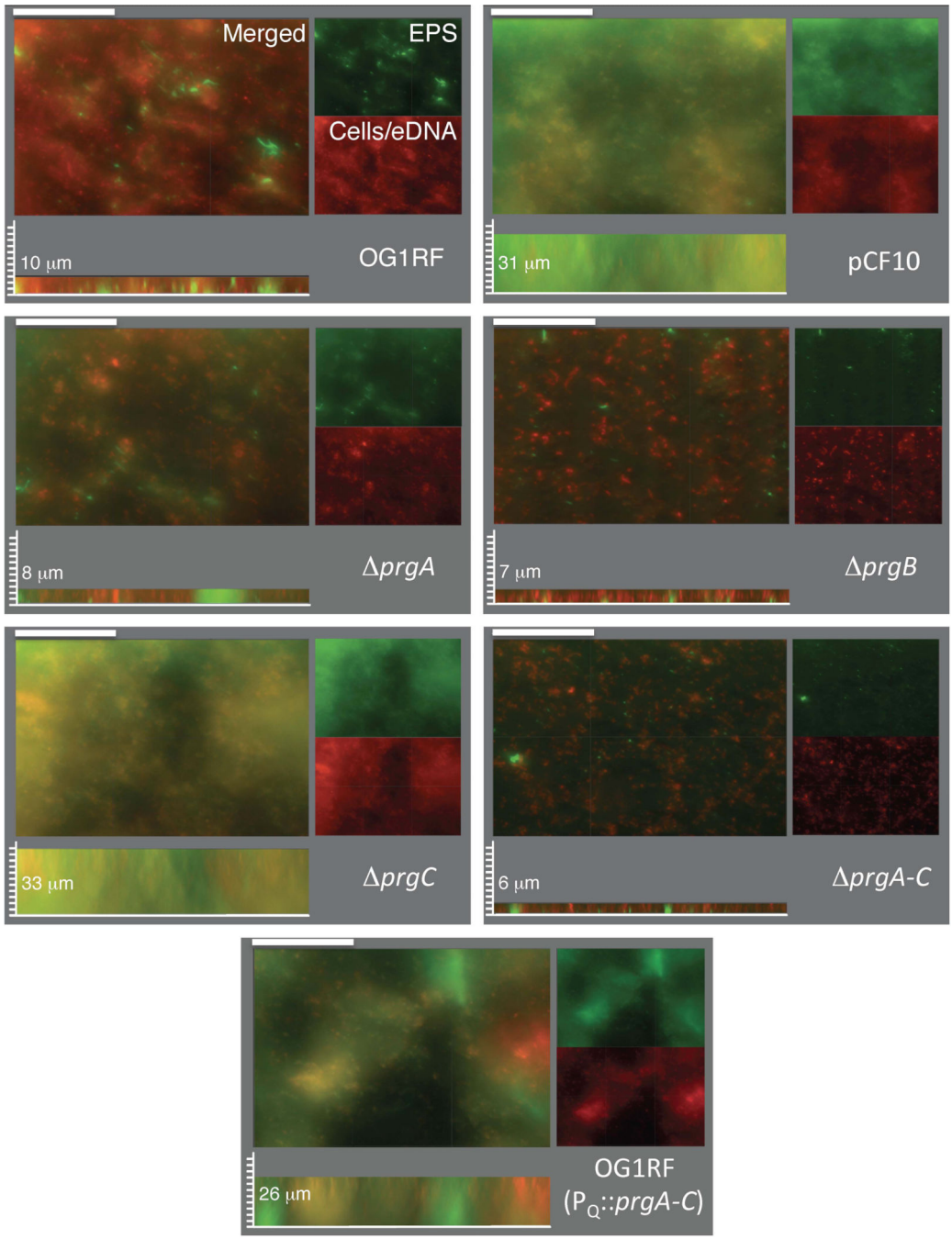

FIG. 5. PrgA and PrgB mediate development of robust, mature biofilms on PMMA coupons

Macroscopic images of biofilms produced by strains inoculated on PMMA coupons at the onset of cCF10 pheromone induction and incubated for 48 h in TSB medium. Cells and eDNA were stained with hexidium iodide (red), extracellular polysaccharide (EPS) was stained with calcofluor white (green). Merged two-color images and corresponding separated color channels of representative 48-h biofilms at 40× magnification are shown; scale bars, 50 μm. Sagittal views are shown depicting biofilm thicknesses with measured

values shown in μM; scale bars, 3.125 μm. Strains: OG1RF lacking or carrying pCF10 or pINY1801 (P_Q::*prgA-C*) or the pCF10 variants Δ*prgA-C*, Δ*prgA*, Δ*prgB*, or Δ*prgC*.

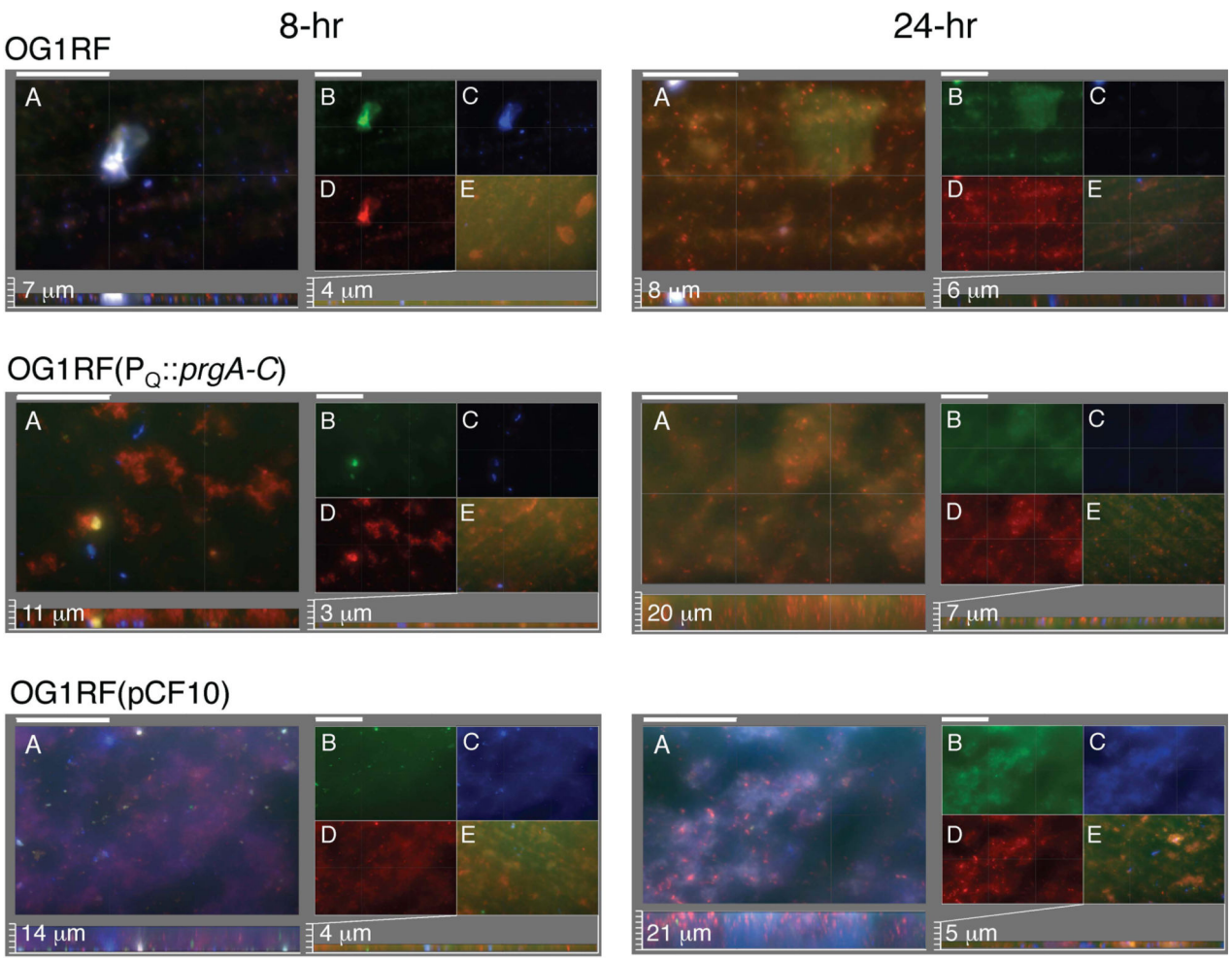

FIG. 6. The Prg proteins and eDNA mediate early biofilm development

Macroscopic images of sections of biofilms produced by strains inoculated on PMMA coupons at the onset of cCF10 pheromone induction and incubated for 8 h (left panels) and 24 h (right panels) in TSB medium. Intact cells were stained with hexidium iodide (HI, red), eDNA and lysed cells were stained with GelGreen (green), and EPS was stained with calcofluor white (blue). Panels A-E are identified for the 8 h biofilm images of strain OG1RF and similarly-arranged for the other strains and time points analyzed. Panels A: Three color-merged images; scale bars, 50 μm. Below: Sagittal projections showing biofilm thicknesses with measured values shown in μM; scale bars, 3.125 μm. Panels B-D: Matched sets to biofilms in panel A showing separate staining of (B) GelGreen, (C) HI, (D) calcofluor white. Panels E: Biofilms were treated with DNase at the onset of pheromone induction, stained with GelGreen, HI, and calcofluor white, and the three-color merged images are presented, with biofilm thicknesses presented below with scale bars equivalent to those used in Panel A. Strains: OG1RF, (OG1RF(pCF10), OG1RF(pINY1801) which expresses P$_Q$::*prgA-C*.

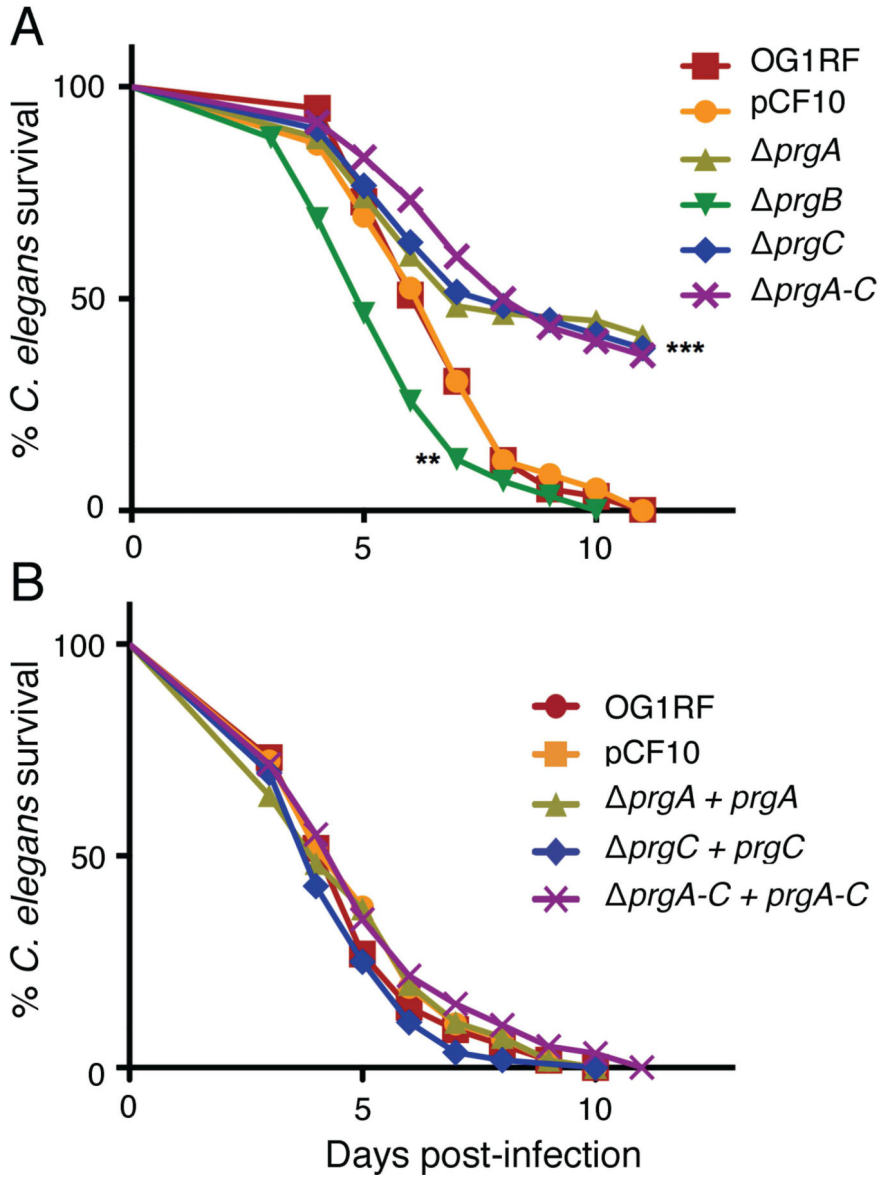

FIG. 7. PrgA and PrgC are important virulence factors in the *C. elegans* infection model

Survival of *C. elegans* fed on **(A)** *E. faecalis* OG1RF without or with pCF10 or the Δ*prg* plasmid variants listed, **(B)** pCF10Δ*prgA*, pCF10Δ*prgC*, pCF10Δ*prgA-C* complemented with their respective genes expressed from the P_Q promoter carried on plasmids pMB5, pMB7, or pINY1801. Survival was scored daily and the differences in survival from the control (pCF10) are shown for pCF10Δ*prgB* (***P*<0.01) and for pCF10Δ*prgA*, pCF10Δ*prgC*, and pCF10Δ*prgA-C* (****P*<0.001). Each experiment was repeated in triplicate at least 3 times and the average values for a representative experiment are shown.

TABLE 1

Plasmids used in this study.

Plasmid	Relevant features	Source or Reference
pCF10	Tet^r, pheromone inducible conjugative plasmid	(Dunny *et al*, 1981)
pCF10Δ*oriT*	Tet^r, pCF10 with a 54-bp deletion within *oriT*	(Staddon *et al.*, 2006)
pCF10Δ*prgA*	Tet^r, pCF10 deleted of *prgA*	This study
pCF10Δ*oriT*Δ*prgA*	Tet^r, pCF10 deleted of *oriT* and *prgA*	This study
pCF10-8, here designated pCF10Δ*prgB*	Tet^r, pCF10 deleted of *prgB*	(Chuang-Smith *et al.*, 2010)
pCF10Δ*prgC*	Tet^r, pCF10 deleted of *prgC*	This study
pCF10Δ*oriT*Δ*prgC*	Tet^r, pCF10 deleted of *oriT* and *prgC*	This study
pCF10Δ*prgA-C*	Tet^r, pCF10 deleted of *prgA, prgB, prgU and prgC*	This study
pDLP278p23	Spc^r, pDL278 with *L. lactis* constitutive promoter P_{23}	(Chen *et al.*, 2007)
pMB2	Spc^r, pDL278p23 expressing P_{23}::prgA	This study
pMB3	Spc^r, pDL278p23 expressing P_{23}::prgB	This study
pMB4	Spc^r, pDL278p23 expressing P_{23}::prgC	This study
pCIE	Cm^r, cCF10 inducible P_Q expression vector	Dunny Lab
pMB5	Cm^r, pCIE expressing P_q::*prgA*	This study
pMB6	Cm^r, pCIE expressing P_Q::*prgB*	This study
pMB7	Cm^r, pCIE expressing P_Q::*prgC*	This study
pINY1801	Cm^r, fragment of pCF10 cloned in shuttle vector pWM401; expresses P_q::*prgA-C*	(Christie *et al.*, 1988)